Multiple roles for protein kinase C in gastropod embryogenesis

Journal:	*Cell and Tissue Research*
Manuscript ID:	CTR-14-0716.R2
Manuscript Type:	Short Communication
Date Submitted by the Author:	n/a
Complete List of Authors:	Zukaite, Vainora; Kingston University, School of Life Sciences Cook, Richard; Kingston University, School of Life Sciences Walker, Anthony; Kingston University, School of Life Sciences
Keywords:	Protein kinase signalling, Gastropod embryogenesis, Embryo gliding, Embryo rotation, Embryo heartbeat

The final publication is available at Springer via http://dx.doi.org/10.1007/s00441-015-2288-3

SHORT COMMUNICATION

Multiple roles for protein kinase C in gastropod embryogenesis

Vainora Zukaite, Richard T. Cook, Anthony J Walker

School of Life Sciences, Kingston University, Penrhyn Road, Kingston upon Thames, Surrey, KT1 2EE, UK

Anthony J Walker (corresponding author)
e-mail: t.walker@kingston.ac.uk
Tel: +44 (0)208 417 2466

Abstract

Protein kinase C (PKC) contributes to the correct development of organisms, but its importance to embryogenesis of molluscs is not yet known. We report here that PKC activation is cyclic within early developing embryos of the gastropod snail *Lymnaea stagnalis* and that activation with phorbol myristate acetate (PMA) results in disorganised and developmentally arrested embryos within 24 h. Moreover, chronic modulation of PKC activation by PMA or by the PKC inhibitor GF109203X in early embryos results in altered rotation and gliding behaviours, and heartbeat during development. Finally, dis-regulation of PKC activity during early development significantly increased the duration to hatching. Our findings thus support novel roles for PKC in *L. stagnalis* embryos, in several physiological contexts, providing further insights into the importance of protein kinases to gastropod development in general.

Keywords: Protein kinase signalling; Gastropod embryogenesis; Embryo gliding; Embryo rotation; Embryo heartbeat.

Introduction

Protein kinase C (PKC) helps co-ordinate correct embryogenesis of many organisms including fruit flies, sea urchins, nematodes, and mice (Cox et al. 2001; Dickey-Sims et al. 2005; Gallicano et al. 1997; Tabuse et al. 1998; Wu et al. 1998). For example, when sea urchins are treated with the PKC inhibitor chelerthrine from the mesenchyme blastula stage onwards they display gastrulation defects and extensive apoptosis (Dickey-Sims et al. 2005), and in *Caenorhabditis elegans*, ablation of atypical PKC3 in oocytes results in disorganized developmentally arrested embryos (Wu et al. 1998). In mammals 10 PKCs exist including PKCβI/βII, which arises from alternate gene splicing. These PKCs are separated into structurally/functionally distinct groups according to their regulatory domains. Thus, conventional PKCs (cPKCs; PKCα, PKCβI/βII, and PKCγ) are diacylglycerol (DAG) sensitive and Ca^{2+}-responsive, novel PKCs (nPKCs; PKCδ, PKCε, PKCη, and PKCθ) are DAG sensitive but are unresponsive to Ca^{2+}, whereas atypical PKCs (aPKCs; PKCζ and PKCι, λ-murine) are insensitive to both DAG and Ca^{2+} (Rosse et al. 2010). Given the incomplete/draft nature of mollusc genomes it remains unclear how many PKC isotypes exist in molluscs.

The extent to which PKC orchestrates developmental processes in molluscs remains unknown. This contrasts with extracellular signal-regulated kinase (ERK), which has been found to have a role in the dorsal (D) quadrant organizer cell 3D in molluscs (Henry and Perry 2008; Koop et al. 2007; Lambert and Nagy 2001, 2003), supporting a role for ERK in axis specification. The gastropod pond snail *Lymnaea stagnalis* is a model organism that has particularly been used in developmental biology for example in studying chirality (Shibazaki et al. 2004; Kuroda et al. 2009), development of the nervous system (Voronezhskaya et al. 2004), and shell formation (Hohagen and Jackson 2013; Shimizu et al. 2011). Embryos remain enclosed within their translucent egg capsules throughout development from oviposition to the juvenile stage, hatching as a miniature version of the adult snail. The aim of this study was to investigate PKC activation dynamics during early embryogenesis and identify physiological roles for PKC in gastropod development, using *L. stagnalis* as a model. To our knowledge, this study is the first to explore PKC signalling events during spiralian development.

Materials and methods

Snails

Lymnaea stagnalis were kept in tanks containing filtered (Brimak PO4 filtration unit, Silverline UK) aerated tap water within a temperature-controlled incubator (Sanyo) set on a 12 h light/12 h dark cycle at 21°C. Snails were fed round lettuce and fish food. Egg masses were selected based on the developmental status of their embryos (staged after Filla et al. 2008) as required.

Microscopy analysis of PKC activation within embryos

To study the temporal dynamics of PKC activation within embryos during development, selected embryos at various stages (1- to >24-cell stage) within their capsules were dissected from their egg masses, fixed for 45 min in 3.7% formaldehyde and washed twice in 300 µl PBS. Additionally, 2-cell stage embryos adjacent to one another in the same egg mass (and thus of slightly different age to one another) were removed from the mass and fixed immediately to provide a temporal picture of PKC activation during this developmental phase. Furthermore, in parallel experiments, 2- or 4-cell stage embryos within their egg capsules but dissected from the egg mass were exposed to the PKC inhibitor GF109203X (10 µM; Calbiochem), the PKC activator phorbol myristate acetate (PMA, 10 µM; New England Biolabs (NEB)), or vehicle (water or DMSO (0.1%)), respectively, for various durations prior to fixing to determine the ability of these compounds to modulate PKC activity within embryos. After fixing, embryos were carefully released from their capsules under a dissecting microscope using a scalpel, collected individually using a pipette, and were each transferred to a well of a 24-well tissue culture plate (Nunc) containing 300 µl PBS. Embryos were then permeabilised in 0.1% Triton X-100 in PBS for 40 min, washed with PBS, then incubated for 30 min in 0.1% glycine. After a further wash in PBS, embryos were blocked in 0.4% BSA for 60 min and washed in PBS/Tween 20 (0.1%; PBST) before incubating in rabbit anti-phospho-PKC (βII Ser 660) (Cell Signalling Technology, NEB) and mouse anti-β-tubulin cy3 (Sigma-Aldrich) primary antibodies (each 1/100 in blocking buffer) for 72 h while rocking at 4°C. Afterwards, embryos were washed 5 times (twice 20 min, thrice 5 min each) with PBST and incubated in FITC-conjugated anti-rabbit Alexa Fluor 488 secondary antibodies (1/500 in blocking buffer) overnight. All samples were then washed a further 4 times with PBST prior to carefully mounting onto slides in Slow Fade Gold anti-fade reagent (with DAPI). Cover slips were sealed with clear nail varnish and

specimens visualised under a Leica TCS-SP2-AOBS laser scanning confocal microscope using a 20x dry objective and images captured. Any background signal received from the negative controls (i.e. embryos incubated only in secondary antibody) was negated from that of the positive samples by reducing the photomultiplier tube voltage, which was then kept constant for observations.

Effect of PKC modulation on developmental parameters

To establish long-term effects of GF109203X or PMA on developing *L. stagnalis* embryos, sibling 2- or 4-cell stage embryos within their capsules were dissected from eggs masses and randomly placed individually into wells of a 24-well tissue culture plate containing either PMA or GF109203X at different concentrations (0.01 – 10 μM), water, or DMSO (vehicle control for PMA, 0.1%); all solutions and compounds were changed daily for the duration of the experiment. The effects of PMA or GF109203X on the following parameters were then observed at the same time each day whilst embryos were developing: 1) rotation, the number of complete turns of the embryo within the capsule; 2) gliding, the number of complete circles performed around the capsule by an embryo moving along the inner surface of the egg capsule wall; and 3) heartbeat. Ten embryos were used per treatment, and each parameter was observed for 3 min. The embryos were maintained at 21°C on a 12 h light/12 h dark cycle. Where appropriate, images were captured under a Motic inverted light microscope with a Moticam 5 digital camera system.

Next, to determine any potential immediate (rather than developmental) effects of PKC modulation on rotation, gliding and heartbeat, trochophore/veliger/ adult-like form stage embryos were collected and exposed to PMA (1 or 10 μM), GF109203X (1 or 10 μM), DMSO (vehicle) or water for 5 – 30 min and observed; a 60 min time point was also included for GF109203X. These embryo stages were used because they display rotation, gliding and heartbeat (Filla et al. 2008); care was taken to ensure that all embryos used to study a particular parameter were of a similar developmental stage.

To determine the effects of PMA or GF109203X on hatching, sibling 2-cell stage embryos (incubated at 0.01 and 0.1 μM, or 0.01 – 10 μM, respectively) or early veliger stage embryos (incubated at 10 μM) isolated from separate egg masses were exposed to these compounds. Embryos in 24-well tissue culture plate wells were maintained at 21°C, 12 h light/12 h dark cycle, and PMA, GF109203X, DMSO

(vehicle for PMA), or water were changed daily; 10 embryos were used per treatment and the experiment was repeated twice.

Statistical analysis

Raw phenotype data was collected from a series of independent experiments and was tested to ascertain if it was normally distributed using the Shapiro-Wilk test; not normally distributed data was transformed (square-rooted). Data was then analysed by analysis of variance (ANOVA) and post-hoc multiple-comparison tests (Fisher's) using SPSS. Duration to hatching data were analysed using the Kaplan-Meier curves and the log-rank test was used to deduce statistical significance between treatments (Rich et al. 2010). In all cases data for embryos treated with GF109203X and PMA was compared to that for control embryos in water and DMSO, respectively.

Results and Discussion

Analysis of PKC activation within early embryos

Previously we validated anti-phospho PKC (βII Ser660) antibodies for detecting exclusively phosphorylated, activated, PKC in adult *L. stagnalis* (Plows et al. 2004, 2005; Walker and Plows 2003; Wright et al. 2006). These antibodies detect PKCα, βI, βII, δ, ε, η and θ isotypes only when phosphorylated at a residue homologous to Ser660 of human PKCβII that is essential for activation (Behn-Krappa and Newton 1999). In both adults and hatchling *L. stagnalis* the antibodies detect a PKC with molecular mass of ~85 kDa. Here, we used these antibodies to determine the dynamics of PKC activation in gastropod early embryos. In all cases, embryos that were incubated only in secondary antibodies displayed negligible fluorescence (data not shown). Across each of at least five replicate experiments, phosphorylated (activated) PKC was found in early embryos of different cell stages (1- to >24-cell stage) from within the same or different egg masses; however, the extent of activation within embryos varied (Fig. 1a-h). Thus embryos of similar or different developmental stages displayed inconsistent levels of phosphorylated PKC with some positively stained and others not, suggesting a dynamic cycle of PKC signalling. Consequently, 2-cell embryos adjacent to one another in the same egg

mass (and thus differing slightly in age) were stained and imaged, revealing a transient PKC activation within embryos of the same cell stage during development (Fig. 1i-p). A similar transient pattern of activation was observed for 4-cell stage embryos adjacent in an egg mass although the PKC signal intensity was less apparent (data not shown). Further observation of embryos demonstrated that when undergoing division, 2-cell embryos possessed activated PKC in the dividing zygote, including in the nuclear region (Fig. 1q, r); inspection of individual serial optical z-sections revealed that activated PKC did not directly associate with the microtubule network in the nucleus. In this context, recently, an aPKCζ-like protein was found to localize to the microtubule network of early *L. stagnalis* embryos during cell division and to associate with the polarity protein Par6 (Homma et al. 2011); in *C. elegans* embryos, interaction between aPKC and Par6 is important to polarity establishment and Par6 cortical localization (Li et al. 2010). Given its sensitivity to GF109203X, the activated *L. stagnalis* PKC detected in the current study is likely most similar to a cPKC isotype, as also deduced for adult snails (Walker and Plows 2003; Wright et al. 2006). Although it is currently unknown how many PKC isotypes are present in *L. stagnalis*, isoform-specific PKC expression/localisation has been shown to alter during early development of mammal embryos (Kalive et al. 2010), whereby 2-cell stage embryo nuclei are enriched with PKC α,δ, and ζ, whereas at the 4-cell stage PKCζ is found at the nuclear periphery (Kalive et al. 2010). As in the current study, the use of antibodies that detect exclusively the activated form of a kinase can yield valuable knowledge of kinase activation rather than simply expression during development, and other anti-active antibodies (including that for PKCζ) should be characterised for use in *L. stagnalis* and other molluscs and invertebrates.

GF109203X inhibits, and PMA activates, PKC in adult *L. stagnalis* defence cells (Walker and Plows 2003; Wright et al. 2006) and GF109203X also attenuates PKC signalling in *L. stagnalis* neurons (van Soest et al. 2000). GF109203X acts as a competitive inhibitor for the ATP binding site of PKC which blocks PKC autophosphorylation at Ser660 (Motley et al. 2002) and PMA acts as a DAG analogue. These compounds were therefore tested for their ability to modulate PKC activation, with 2-cell and 4-cell embryos used for GF109203X and PMA treatments, respectively, due to greater PKC activation generally seen in 2-cell embryos and *vice versa*. Treatment with PMA for 5 or 10 min (Fig. 2b, c) increased PKC phosphorylation in embryos in contrast to that seen in DMSO controls (Fig. 2a). In contrast, treatment with GF109203X reduced PKC activation over time (Fig. 2d-f). Because PKC activation in embryos appears transient, it could be argued that the

observed effects of PMA/GF109203X treatment might be due to developmental fluctuations in PKC activity. However, across five separate replicate experiments over 30 embryos were analysed for each treatment and in all cases PMA resulted in increased staining, whereas GF109203X resulted in a substantial reduction or complete loss of activated PKC, demonstrating the ability of these compounds to either activate or inhibit PKC in intact embryos, respectively.

Multiple effects of PKC modulation on embryo phenotype and behaviour

We next explored the effects of PKC modulation on embryo development. Initially, 2- or 4-cell embryos were removed from a single egg mass and were exposed to PMA, GF109203X, or vehicle at differing concentrations for 24 h. Whereas no obvious developmental aberrations were seen after 24 h with GF109203X (0.01 – 10 μM) or with low (<1 μM) doses of PMA, incubation with either 1 or 10 μM PMA resulted in deformed embryos with disrupted tissue patterning and no discernable axes (Fig. 2g-k); protrusions of yolky cells were also often apparent. These findings support the notion that while cPKC-like activation seems non-essential for early embryogenesis and correct patterning of *L. stagnalis*, sustained cPKC activation might be detrimental and needs to be tightly controlled. In contrast, in *C. elegans* ablation of aPKC (PKC-3) function results in disorganized and developmentally arrested embryos (Wu et al. 1998) and in *Drosophila melanogaster* RNA interference (RNAi) of the nPKCδ homologue PKC98E affects embryo development along the dorso-ventral axis (Tremmel et al. 2013).

Because 1 or 10 μM PMA severely impacted embryogenesis, experiments investigating effects of chronic PMA treatment on physiology of developing embryos were done using lower PMA doses (0.01 or 0.1 μM), whereas GF109203X was used at 0.1 – 10 μM. Rotation of embryos was determined from day three (when at veliger stage) until they ceased rotating. Two factor ANOVA revealed an overall effect of day ($P \leq 0.001$) and treatment ($P \leq 0.01$) on rotation; slower rotation was seen on days 3 and 7/8 compared with days 4-6 ($P \leq 0.001$) irrespective of treatment (Fig. 3a, d). However, 0.01 or 0.1 μM PMA significantly increased rotation ($P \leq 0.001$) when compared to DMSO controls, with 0.1 μM having the greatest effect, particularly on days 5 and 7 where increases of ~150% and ~400% were seen compared to DMSO ($P \leq 0.01$; Fig. 3a). On the other hand, each dose of GF109203X attenuated rotation on days 4 and 5 ($P \leq 0.001$) by up to ~29%, whereas surprisingly 0.1 – 10 μM GF109203X increased rotation on day 6 ($P \leq 0.05$) (Fig. 3d). Heartbeat, observable

from day 6, was also affected by day ($P \leq 0.001$) and treatment ($P \leq 0.001$). PMA (0.01 or 0.1 μM) enhanced heartbeat on the majority of days when compared to DMSO-treated sibling embryos (Fig. 3b). In contrast, chronic GF109203X treatment caused reduced embryo heartbeat, particularly on days 9 -11 ($P \leq 0.001$), with the greatest reduction (~45%) seen with 1 μM GF109203X on day 11 ($P \leq 0.001$) (Fig. 3e). Finally, gliding was observed over 4 – 5 days starting once embryos approached the end of metamorphosis. Again, two factor ANOVA revealed a significant overall effect of day ($P \leq 0.001$) and treatment ($P \leq 0.05$) on gliding. In control embryos gliding on day 8 was greater than on day 7 ($P \leq 0.05$), but declined again by day 10/11 (Figs. 3c, f). However, post-hoc multiple comparison tests revealed that the treatment effect did not depend on day of observation; thus PMA did not effect gliding on any one day when compared to controls (Fig. 3c). In contrast, chronic exposure to 0.1 μM or 10 μM GF109203X resulted in a significant 49% ($P \leq 0.05$) and 57% ($P \leq 0.001$) reduction in embryo gliding, respectively, on day 8 (Fig. 3f).

In an attempt to further establish whether effects of PMA or GF109203X on rotation, heartbeat and gliding were due to altered physiology during development or were due to short-term exposure to the compounds, embryos were incubated in GF109203X or PMA (each at 1 μM or 10 μM) for up to 60 min and rotation, heartbeat and gliding determined every 5 or 10 min and compared to that of sibling embryos in water and DMSO. ANOVA revealed that mean rotation and heartbeat were unaffected by GF109203X or PMA at any time point, or by either dose. However, 1 μM PMA increased gliding by ~105% at 30 min and 10 μM PMA increased gliding by between 90 % and 230 % after 10, 20 and 30 min exposure ($P \leq 0.01$; data not shown) when compared to DMSO controls. On the other hand, gliding rates of GF109203X treated embryos were not significantly different to those of control sibling embryos at any time observed over the 60 min treatment period.

Ciliary motion drives rotation in *L. stagnalis* embryos (Voronezhskaya et al. 1999) and PKC modulates ciliary beat frequency (CBF) in mammals (Salathe 2007) and mediates serotonin (5-HT) stimulated CBF in embryo epithelial cells of the gastropod *Helisoma trivolvis* (Chistopher et al. 1999). In addition, gliding in *Lymnaea* results from combined action of the cilia and phasic smooth muscles in the sole of the foot (Pavlova 2010, 2013). Moreover, smooth muscle contraction, including that of the heart, relies upon co-ordinated PKC activity (Andrea and Walsh 1992; Salamanca and Khalil 2005). Thus, although further experiments are required to unravel the complex effects of PKC modulation on these parameters during *L. stagnalis* embryogenesis, the results in this study support the hypothesis that rotation

and heartbeat, and to some extent gliding, result from changes mediated by PMA and GF109203X treatment during development, rather than from short-term treatment alone.

Effect of PKC modulation on duration to hatching

Although hatching of *L. stagnalis* embryos can lack synchrony when embryos remain in the egg mass, hatching is largely synchronous when eggs are isolated from the mass (Marois and Croll 1991) as done in the current study. Kaplan-Meier curves and log-rank tests of hatching data obtained from experiments with isolated early cleavage stage (2- or 4-cell) embryos revealed that chronic PMA ($P \leq 0.01$) (Fig 4a) or GF109203X ($P \leq 0.001$) (Fig. 4b) treatment delayed hatching when compared to control embryos, with only 0.01 μM PMA being without effect. On day 12, 60% fewer embryos hatched following 0.1 μM PMA treatment than with vehicle (DMSO) (Fig. 4a) and 50% and 90% less hatched when exposed to 0.01 μM and 0.1/1 μM GF109203X, respectively (Fig. 4b). Furthermore, a small proportion, 10% and 20%, of embryos died following chronic treatment with 0.1 μM PMA and 10 μM GF109203X, with death occurring on days 14 and 13, respectively. Finally, a further experiment was undertaken to ascertain whether hatching was affected when later (veliger) stage sibling embryos were chronically exposed to 10 μM PMA or 10 μM GF109203X. While 10 μM GF109203X did not delay hatching or kill embryos, 10 μM PMA caused 70% death within three days, without significantly affecting the hatching time of survivors (data not shown). This difference in duration to hatching between early and later embryos in the face of PKC modulation, supports the idea that that blocking or promoting PKC activity alters the molecular events that influence normal development leading to increased developmental periods, possibly influenced by secondary effects of cilia motion and muscle activity.

Given the relative paucity of research into protein kinases during mollusc development it is hoped that the founding experiments detailed here, perhaps coupled with RNAi (Knight et al. 2011) and embryo culture outside the capsule (Dickinson and Croll 2001) will help provide a framework for further work to functionally elucidate signalling during processes such as tissue patterning in this important group of animals.

Acknowledgements

We are grateful to Richard Giddens of Kingston University for his support using the confocal laser scanning microscope.

References

Andrea JE, Walsh MP (1992) Protein-kinase-C of smooth-muscle. Hypertension 20:585-595

Behn-Krappa A, Newton AC (1999) The hydrophobic phosphorylation motif of conventional protein kinase C is regulated by autophosphorylation. Current Biol 9:728-737

Christopher KJ, Young KG, Chang JP, Goldberg JI (1999) Involvement of protein kinase C in 5-HT-stimulated ciliary activity in *Helisoma trivolvis* embryos. J Physiol 515:511-522

Cox DN, Seyfried SA, Jan LY, Jan YN (2001) Bazooka and atypical protein kinase C are required to regulate oocyte differentiation in the *Drosophila* ovary. *Proc Natl Acad Sci USA* 98:14475-14480

Dickinson AJG, Croll RP (2001) A culture technique for experimental studies of embryonic development in the pond snail *Lymnaea stagnalis*. Invert Reprod Develop 40:39-48

Dickey-Sims C, Robertson AJ, Rupp DE, McCarthy JJ, Coffman JA (2005) Runx-dependent expression of PKC is critical for cell survival in the sea urchin embryo. BMC Biol 3:18

Filla A, Hiripi L, Elekes K (2008) Role of aminergic (serotonin and dopamine) systems in the embryogenesis and different embryonic behaviours of the pond snail, *Lymnaea stagnalis*. Comp Biochem Physiol Pt C 149:73-82

Gallicano GI, Yousef MC, Capco DG (1997) PKC – a pivotal regulator of early development. BioEssays 19:29-36

Henry JJ, Perry KJ (2008) MAPK activation and the specification of the D quadrant in the gastropod mollusc, *Crepidula fornicata*. Dev Biol 313:181-195

Hohagen J, Jackson DJ (2013) An ancient process in a modern mollusc:early development of the shell in *Lymnaea stagnalis*. BMC Dev Biol 13:27

Homma T, Shimizu M, Kuroda R (2011) The polarity protein Par6 is coupled to the microtubule network during molluscan early embryogenesis. Biochem Biophys Res Comm 404:173-178

Kalive M, Faust JJ, Koneman BA, Capco DG (2010) Involvement of the PKC family in regulation of early development. Mol Reprod Dev 77:95-104

Koop D, Richards GS, Wanninger A, Gunter HM, Degnan BM (2007) The role of MAPK signalling in patterning and establishing axial symmetry in the gastropod *Haliotis asinina*. Dev Biol 311:200-212

Knight M, Miller A, Scaria P, Woodle M, Ittiprasert W (2011) Polyethyleneimine (PEI) mediated siRNA gene silencing in the *Schistosoma mansoni* snail host, *Biomphalaria glabrata*. PLoS Negl Trop Dis 5: e1212

Kuroda R, Endo B, Abe M, Shimizu M (2009) Chiral blastomere arrangement dictates zygotic left-right asymmetry pathway in snails. Nature 462:790-794

Lambert JD, Nagy LM (2001) MAPK siginaling by the D quadrant embryonic organizer of the mollusc *Ilyanassa obsoleta*. Development 128:45-56

Lambert JD, Nagy LM (2003) The MAPK cascade in equally cleaving spiralian embryos. Dev Biol 263:231-241

Li J, Kim H, Aceto DG, Hung J, Aono S, Kemphues KJ (2010) Binding to PKC-3, but not to PAR-3 or to conventional PDZ domain ligand, is required for PAR-6 function in *C. elegans*. Dev Biol 340:88-98

Marois R, Croll RP (1991) Hatching asynchrony within the egg mass of the pond snail, *Lymnaea stagnalis*. Invert Reprod Dev 19:139-146

Motley ED, Kabir SM, Gardner CD, Eguchi K, Frank GD, Kuroki T, Ohba M, Tamakawa T, Eguchi S (2002) Lysophosphatidylcholine inhibits insulin-induced Akt activation through protein kinase C-alpha in vascular smooth muscle cells. Hypertension 39:508-512

Pavlova GA (2010) Muscular waves contribute to gliding rate in the freshwater gastropod *Lymnaea stagnalis*. J Comp Physiol A 196:241-248

Pavlova GA (2013) Sole smooth muscle states determine gliding rate in the freshwater snail *Lymnaea stagnalis*. Biol Bull 225:184-193

Plows LD, Cook RT, Davies AJ, Walker AJ (2004) Activation of Extracellular–signal Regulated Kinase (ERK) is required for phagocytosis by *Lymnaea stagnalis* haemocytes. Biochim Biophys Acta – Mol Cell Res 1692:25-33

Plows LD, Cook RT, Davies AJ, Walker AJ (2005) Carbohydrates that mimic schistosome surface coat components affect ERK and PKC signalling in *Lymnaea stagnalis* haemocytes. Int J Parasitol 35:293-302

Rosse C, Linch M, Kermorgant S, Cameron AJM, Boeckeler K, Parker PJ (2010) PKC and the control of localized signal dynamics. Nat Rev Mol Cell Biol 11:102-112

Rich JT, Neely JG, Paniello RC, Voelker CCJ, Nussenbaum B, Wang EW (2010) A practical guide to understanding Kaplan-Meier curves. Otolaryngology – Head Neck Surg 143:331-336

Salamanca DA, Khalil RA (2005) Protein kinase C isoforms as specific targets for modulation of vascular smooth muscle function in hypertension. Biochem Pharmacol 70:1537-1547

Salathe M (2007) Regulation of mammalian ciliary beating. Annual Rev Physiol 69:401-422

Shibazaki Y, Shimizu M, Kuroda R (2004) Body handedness is directed by genetically determined cytoskeletal dynamics in the early embryo. Curr Biol 14:1462-1467

Shimizu K, Sarashina I, Kagi H, Endo K (2011) Possible functions of Dpp in gastropod shell formation and shell coiling. Dev Genes Evol 221:59-68

Tabuse Y, Izumi Y, Piano F, Kemphues KJ, Miwa J, Ohno S (1998) Atypical protein kinase C cooporates with PAR-3 to establish embryonic polarity in *Caenorhabditis elegans*. Development 125:3607-3614

Tremmel DM, Resad S, Little CJ Wesley CS (2013) Notch and PKC are involved in formation of the lateral region of the dorso-ventral axis in *Drosophila* embryos. PLoS One 8:e67789

Van Soest PF, Lodder JC, Kits KS (2000) Activation of protein kinase C by oxytocin-related conopressin underlies pacemaker current in *Lymnaea* central neurons. J Neurophysiol 84:2541-2551

Voronezhskaya EE, Hiripi L, Elekes K, Croll R (1999) Development of catecholaminergic neurons in the pond snail *Lymnaea stagnalis*: I. embryonic development of dopamine-containing neurons and dopamine-dependent behaviors. J Comp Neurol 404:285-296

Voronezhskaya EE, Khabarova MY, Nezlin LP (2004) Apical sensory neurones mediate developmental retardation induced by conspecific environmental stimuli in freshwater pulmonate snails. Development 131:3671-3680

Walker AJ, Plows LD (2003) Bacterial lipopolysaccharide modulates protein kinase C signalling in *Lymnaea stagnalis* haemocytes. Biol Cell 95:527-533

Wright B, Lacchini AH, Davies AJ, Walker AJ (2006) Regulation of nitric oxide production in *Lymnaea stagnalis* defence cells: a role for protein kinase C and extracellular signal-regulated kinase signalling pathways. Biol Cell 98:265-278

Wu SL, Staudinger J, Olsen EN, Rubin CS (1998) Structure, expression, and properties of an atypical protein kinase C (PKC3) from *Caenorhabditis elegans* – PKC3 is required for the normal progression of embryogenesis and viability of the organism. J Biol Chem 273:1130-1143

Figure Legends

Fig. 1 Cyclic PKC activation occurs in *L. stagnalis* embryos during early development. **a-h** Confocal fluorescence micrographs of embryos stained with anti-phospho PKC (Ser660) and AlexaFluor 488 antibodies showing activated PKC (green) within embryos at various (1-cell - >24-cell) stages. **i-p** Confocal fluorescence micrographs of 2-cell stage embryos from the same mass of egg capsules. Embryos were fixed in chronological order from the first (1^{st}) to the last (8^{th}) laid egg observed within the egg mass and were stained for activated PKC (green), and for microtubules (red) with anti-tubulin cy3 conjugated antibodies. **q** Activated PKC (green) during embryo division with microtubule spindle shown (red). **r** Zoom of boxed region shown in '**q**'. In each case, results shown represent those observed from at least 5 independent experiments. Confocal microscopy images are maximum projections of image z-stacks. Bars represent 25 μm.

Fig. 2 Modulation of PKC activation in *L. stagnalis* embryos by PMA or GF109203X, and effects of PMA on development. **a-f** Confocal fluorescence micrographs of embryos stained with anti-phospho PKC (Ser660) and AlexaFluor 488 antibodies showing activation of PKC (green) by PMA, or inhibition by GF109203X within embryos. Embryos were exposed to either 10 μM PMA for 5 or 10 min or 0.1% DMSO vehicle (control), or to 10 μM GF109203X for 5 or 30 min or water (control) prior to fixing and staining with antibodies. **g-k** Effects of 24 h PMA (1 or 10 μM) treatment on embryo development compared with sibling control embryos (0.1 % DMSO). In each case, results shown represent those observed from at least 5 independent experiments. Confocal microscopy images are maximum projections of image z-stacks. Bars represent 25 μm.

Fig. 3 PMA or GF109203X modulate heartbeat and rotation of *L. stagnalis* embryos when administered continuously during development from the early embryo stage. 2-cell or 4-cell stage embryos were treated with **a-c** PMA (0.01 μM or 0.1 μM), 0.1 % DMSO (vehicle), or water, or **d-f** GF109203X (0.01 μM – 10 μM), or water. Rotation, heartbeat and gliding were then observed daily under a dissecting microscope over a 3 min period whilst the embryos were still developing within their egg capsules. Mean values (± S.E.M) are shown. * $P \leq 0.05$, ** $P \leq 0.01$, and *** $P \leq 0.001$ (one-way ANOVA with Fisher post-hoc multiple comparison) when compared to **a-c** DMSO, or **d-f** water

controls; n=10 per treatment and dose, with all embryos randomly selected from five egg masses.

Fig. 4 Effect of GF109203X or PMA on hatching rate of *L. stagnalis* when administered continuously during development from the early embryo stage. 2-cell or 4-cell stage embryos were collected from the same egg mass and were treated with **a** PMA (0.01 µM or 0.1 µM), 0.1 % DMSO (vehicle), or water, or **b** GF109203X (0.01 µM – 10 µM), or water. Numbers of hatched embryos from each treatment were recorded and results are expressed as mean values; n=10 per treatment and dose. Kaplan-Meier analysis/log rank test was applied to the data to determine significant differences between duration to hatching curves: ** $P \leq 0.01$ and *** $P \leq 0.001$ for treatments when compared to **a** DMSO or **b** water curves.

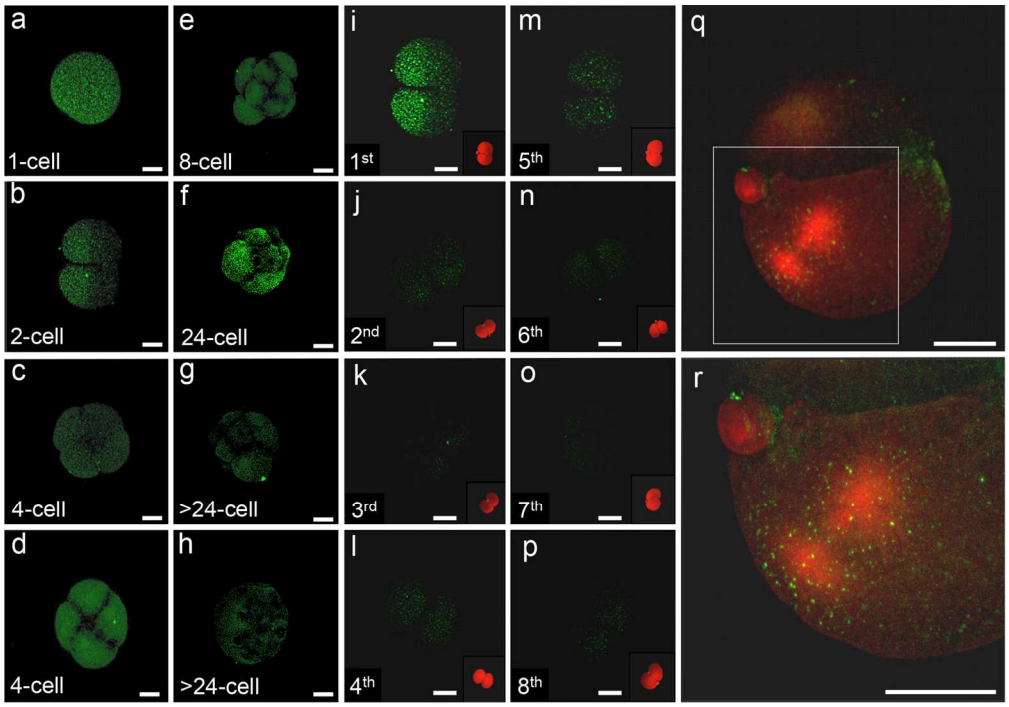

Figure 1
173x121mm (300 x 300 DPI)

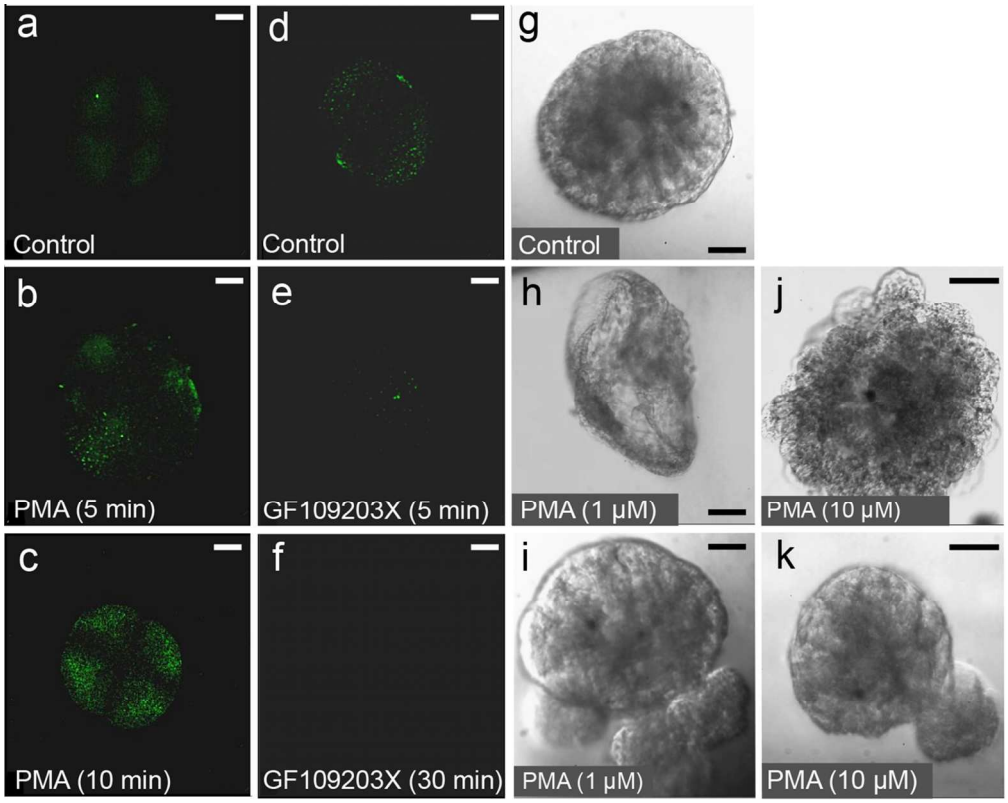

Figure 2
129x102mm (300 x 300 DPI)

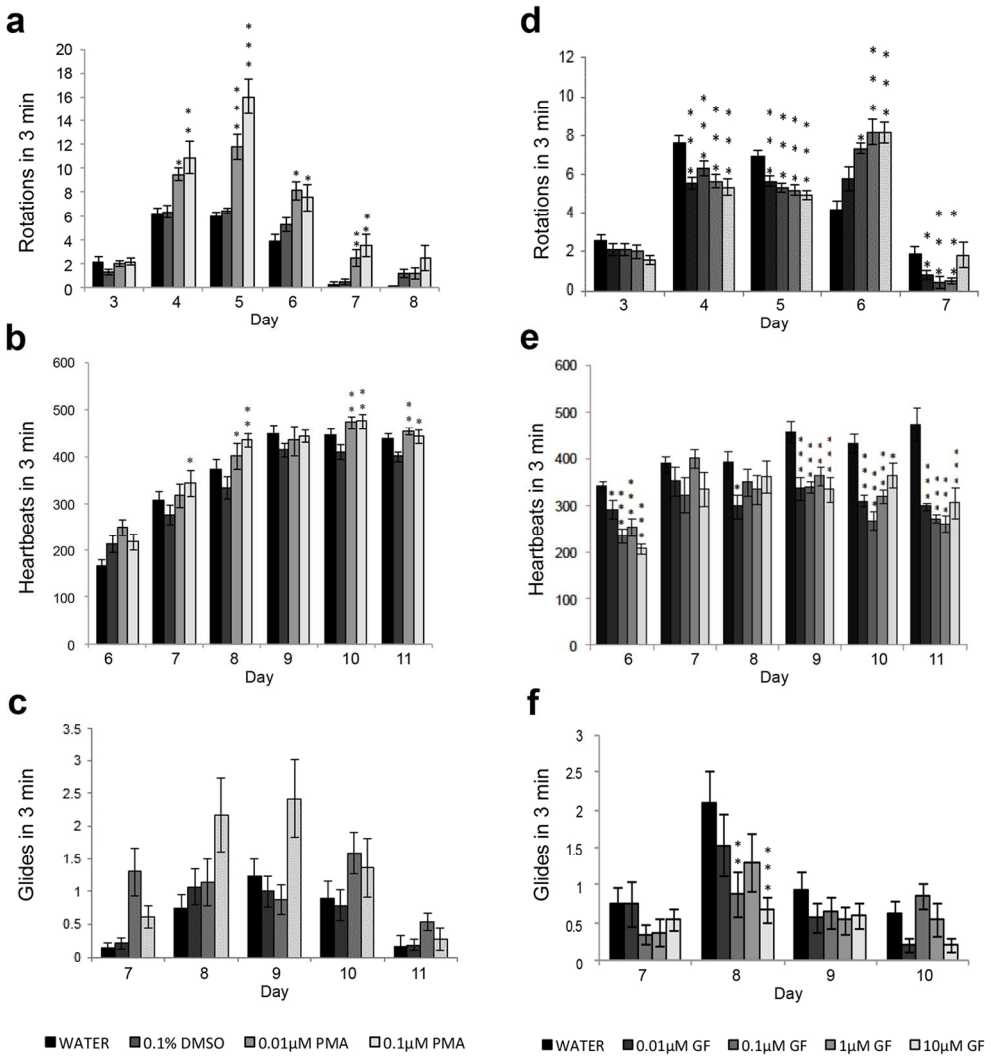

Figure 3
129x137mm (300 x 300 DPI)

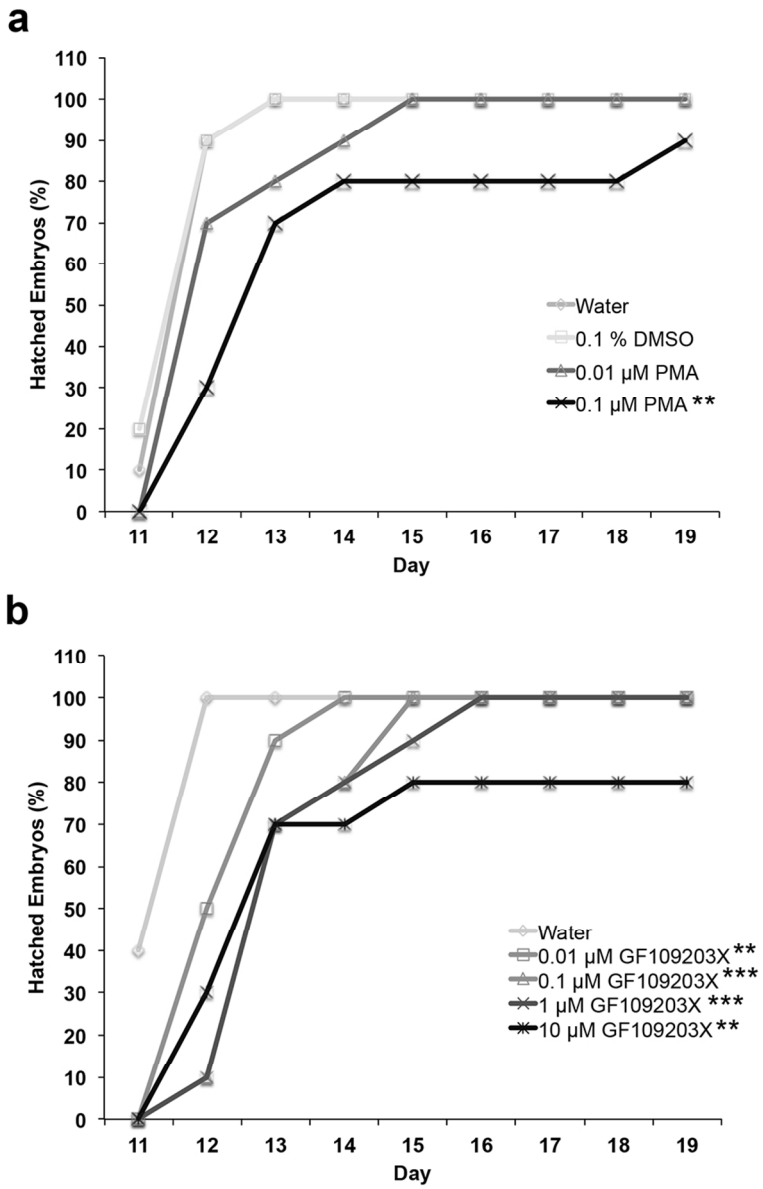

Figure 4
83x129mm (300 x 300 DPI)